Chem. Phys. **120**, 439 (1988).
22. S. G. Boxer, R. A. Goldstein, D. J. Lockhart, T. R. Middendorf, L. Takiff, *J. Phys. Chem.* **93**, 8280 (1989).
23. R. Reich and S. Schmidt, *Ber. Bunsenges. Phys. Chem.* **76**, 589 (1972).
24. T. Kakitani, B. Honig, A. R. Crofts, *Biophys. J.* **39**, 57 (1982).
25. M. Symons and C. Swysen, *Biochim. Biophys. Acta* **723**, 454 (1983).
26. B. Chance and L. Smith, *Nature* **175**, 803 (1955); B. Chance, *Brookhaven Symp. Biol.* **11**, 74 (1958).
27. J. B. Jackson and A. R. Crofts, *FEBS Lett.* **4**, 185 (1969).
28. R. Reich, R. Scheerer, K.-U. Sewe, H. T. Witt, *Biochim. Biophys. Acta* **449**, 285 (1976); B. G. de Grooth and J. Amesz, *ibid.* **462**, 237 (1977); B. G. de Grooth, H. J. van Gorkom, R. F. Meiburg, *ibid.* **589**, 299 (1980).
29. M. Symons *et al.*, *ibid.* **462**, 706 (1977).
30. W. Junge and J. B. Jackson, in *Photosynthesis.* Vol. 1, *Energy Conservation in Plants and Bacteria*, Govindjee, Ed. (Academic Press, New York, 1982), pp. 589–646; W. Crielaard, K. J. Hellingwerf, W. N. Konings, *Biochim. Biophys. Acta* **973**, 205 (1988).
31. Samples that are artificially oriented by insertion into a lipid bilayer or in a Langmuir-Blodgett film are typically oriented axially, not uniaxially, relative to a unique field direction defined by a transmembrane potential. Hence, two populations with chromophore dipole moments having projections parallel and antiparallel to the field are present. So long as $\Delta\mu_A \cdot F_{int}$ (the Stark splitting) is comparable to or smaller than the inhomogeneous linewidth (nearly always the case), then ΔA should depend quadratically on the applied field if equal parallel and antiparallel orientational populations are present (D. J. Lockhart and S. G. Boxer, unpublished results). An isotropic sample is just the extension to all possible parallel and antiparallel orientational populations.
32. An interesting complication could arise if the applied field due to the transmembrane potential or charge separation reaction affected the distribution of matrix fields that induce the permanent dipole moment difference in the carotenoid.
33. We thank H. Frank and C. Violette for providing samples and advice, which were indispensable to this work. This work was supported by a grant from the National Science Foundation Biophysics Program. M.A.S. is a Medical Scientist Training Program (NIH) trainee supported by grant GM07365 from the National Institute of General Medical Sciences.

25 July 1990; accepted 12 October 1990

Fibroblast Growth Factor Receptors from Liver Vary in Three Structural Domains

JINZHAO HOU, MIKIO KAN, KERSTIN MCKEEHAN, GEORGE MCBRIDE, PAMELA ADAMS, WALLACE L. MCKEEHAN*

Changes in heparin-binding fibroblast growth factor gene expression and receptor phenotype occur during liver regeneration and in hepatoma cells. The nucleotide sequence of complementary DNA predicts that three amino-terminal domain motifs, two juxtamembrane motifs, and two intracellular carboxyl-terminal domain motifs combine to form a minimum of 6 and potentially 12 homologous polypeptides that constitute the growth factor receptor family in a single human liver cell population. Amino-terminal variants consisted of two transmembrane molecules that contained three and two immunoglobulin-like disulfide loops, as well as a potential intracellular form of the receptor. The two intracellular juxtamembrane motifs differed in a potential serine-threonine kinase phosphorylation site. One carboxyl-terminal motif was a putative tyrosine kinase that contained potential tyrosine phosphorylation sites. The second carboxyl-terminal motif was probably not a tyrosine kinase and did not exhibit the same candidate carboxyl-terminal tyrosine phosphorylation sites.

THE HEPARIN-BINDING FIBROBLAST growth factor (HBGF) family consists of seven related gene products that have a broad spectrum of biological effects on growth and function of a variety of cell types (*1*). Indirect ligand affinity chromatography and immunochemical analyses suggest that transmembrane tyrosine kinase–like molecules similar to the platelet-derived growth factor and the colony-stimulating factor one (*fms*) receptor family [*fms*-like genes (*flg*)] function as HBGF receptors (*2, 3*). HBGF stimulates and inhibits proliferation and secretory functions of cultured rat hepatocytes and differentiated human hepatoma cells. These cells exhibit a heterogeneous population of HBGF receptors with varied affinity for ligand (*4, 5*). Specific forms of the HBGF receptor may be responsible for a subset of the biological effects induced by the HBGF family members. Here we deduce, from the nucleotide sequence of cDNA, the structural features that combine to define a family of HBGF receptors in human liver cells.

We screened 2×10^6 plaques from a λgt11 expression library made from human hepatoma cell (HepG2) mRNA (*4*). Screening was conducted with synthetic oligonucleotide probes designed from the sequence of a partial human endothelial cell *flg* cDNA (*6*) and yielded five positive clones. Two 2.6-kb cDNAs, a1 and b2 (Fig. 1A), were 98% and 93% similar in nucleotide and deduced amino acid (aa) sequence, respectively (Fig. 1B). The a1 clone had a type 1 COOH-terminus and was identical to the partial human endothelial *flg* cDNA (*6*), except for a single base pair substitution (T to C), which caused a Val to Ala change in an extracellular immunoglobulin (IgG)-like loop structure (Fig. 1). The b2 clone differed from *flg* by a 6-bp (AACAGT) (2 aa) deletion in the intracellular juxtamembrane domain, and by a 25-bp insertion (GTGTGGAACCTGAAGGCTCCCCTGG) in the coding sequence for the second kinase consensus sequence in the intracellular domain (Fig. 1, type 2 COOH-terminus). The 25-bp insertion in b2 caused a shift in the reading frame, which produced a short second kinase consensus sequence (24 aa) followed by 44 unique COOH-terminal residues (Fig. 1). The juxtamembrane sequences encoded in the truncated *flg* cDNAs were designated as a (RRQVTVSA) and b (RRQVSA), respectively. The a and b motifs differed in a possible site of phosphorylation by a Ser-Thr protein kinase.

To deduce the NH_2-terminal sequences of *flg*-related gene products from HepG2 cells, we generated a sublibrary of primer-extended cDNA clones in λgt11 with a mixture of 3′-oligonucleotide primers common to a1 and b2 cDNAs (*7*). From the deduced aa sequences of the primer-extended cDNAs, we identified the NH_2-terminal (extracellular) motifs, which contained three (α) and two (β) IgG-like disulfide loops (Fig. 1). The polymerase chain reaction (PCR) (*8*) was used to further characterize heterogeneity in *flg*-related mRNAs in HepG2 cells [see Fig. 1B and (*9*) for primers]. The PCR was carried out with HepG2 first-strand cDNA as the template, a 5′ primer (P1a), which began 67-bp upstream of the common translational initiation site in the α and β cDNAs, and a 3′ primer (P1b), which ended 111-bp downstream from the first 3′ landmark (T/C) that distinguished a1 and b2 cDNAs (Fig. 1A). This yielded cDNA fragments of 1.1, 1.0, and 0.8 kb (Fig. 1A and Fig. 2A, PCR1). Cloning and sequence analysis confirmed that the 1.1- and 0.8-kb fragments encoded the α (three-loop) and β (two-loop) motifs, respectively. The 1.0-kb fragment coded for the identical translation initiation site and the first 30 NH_2-terminal residues in the 1.1- and 0.8-kb fragments. In addition, it contained a unique 144-bp substitution in place of the 267-bp sequence, which encoded the first IgG-like loop of the α motif. The 144-bp insertion was in the same reading frame as the translation initiation site and multiple stop codons, which began 94 bp downstream of the 5′ insertion site (Fig. 1). An alternate candidate translation initiation site

W. Alton Jones Cell Science Center, Inc., 10 Old Barn Road, Lake Placid, NY 12946.

*To whom correspondence should be addressed.

was located 123 bp past the 3′ insertion site of the 144-bp sequence. It preceded an open reading frame that began downstream of a characteristic stretch of acidic residues and upstream of the two IgG-like loop structures, which were common to both α and β extracellular motifs (Fig. 1). This clone also exhibited a deletion of the sequence CGTATG, which was 33 bp upstream of the candidate initiation site and occurred in all clones that encoded the α and β motifs. This third NH_2-terminal motif (γ) exhibited no apparent signal sequence for membrane translocation and, therefore, suggests an intracellular form of the receptor. The single clones of the three PCR1 fragments all contained the T residue present in the b2 cDNA (Fig. 1A).

Generation of a second set of DNA fragments from HepG2 first strand cDNA template with P1a and P2a, a primer that ended at the 3′ end of the first kinase consensus sequence, yielded three cDNA fragments of 1.8, 1.7, and 1.5 kb (Fig. 2A, PCR2). The 1.8-kb insert (two clones) coded for the α motif linked to the b-type juxtamembrane sequence. Analysis of three clones that contained inserts of the 1.5-kb fragment indicated that the β extracellular motif was linked to both the a-type (one clone) and b-type (two clones) juxtamembrane sequences. The PCR conditions were then optimized to yield specific a1-containing cDNA fragments that existed between a common 5′ primer (P3a) and a 3′ primer (P3b) that was specific to the a-type juxtamembrane sequence. Clones of PCR2 DNA fragments (79 of 1.8-kb and 52 of 1.5-kb inserts) (Fig. 2A) were tested by PCR for the presence of the a-type juxtamembrane sequence. Sequence analysis confirmed that HepG2 mRNA encoded both the α and β extracellular motifs combined with the a-type juxtamembrane sequence.

To determine whether the γ NH_2-terminal motif was linked to type a or b juxtamembrane motifs, we specifically amplified the 1.7-kb cDNA fragment from the PCR2 mixture with P2a and a 5′ primer (P2b) that was specific to the 5′ end of the 144-bp insert in the γ cDNA (Fig. 2A, lane 3). Sequence analysis of a single 1.6-kb clone of the purified cDNA fragment indicated that the γ NH_2-terminal motif was linked to the b-type juxtamembrane sequence. This γb clone encoded the 6-bp sequence (CGTATG) upstream of the candidate initiation site. Presence of the 144-bp (γ motif) insert in four additional clones from an independent experiment was confirmed by PCR analysis with another γ-specific 5′ primer (P2c) and common 3′ primer (P2d) (Fig. 2A, lane 4). Two clones yielded cDNA fragments that existed between a common 5′ primer (P3a) and a 3′ primer (P3b) that contained the a-type juxtamembrane motif. Linkage of the γ and a-type motif was verified by sequence analysis.

We next tested whether HepG2 mRNA contained the a- and b-type juxtamembrane motifs linked to the type 1 and type 2 COOH-termini. Cloned 1.0-kb cDNA fragments were generated from HepG2 first strand cDNA template with 5′ primer, P3a, which was 105 bp upstream of the transmembrane coding sequence, and P5a, which was 230 bp downstream of the 25-bp insertion in b2 (Fig. 1). Thirty-six candidate clones that coded for the a-type motif were identified by screening 209 clones with the common 5′ primer P3a and the a-specific 3′ primer P3b. A PCR screen with a 5′ primer (P5b) common to a1 and b2 cDNAs and a 3′ primer (P5c) specific to the unique 25-bp b2 insert, revealed that 17 of the 36 a-type clones contained the type 2 COOH-termi-

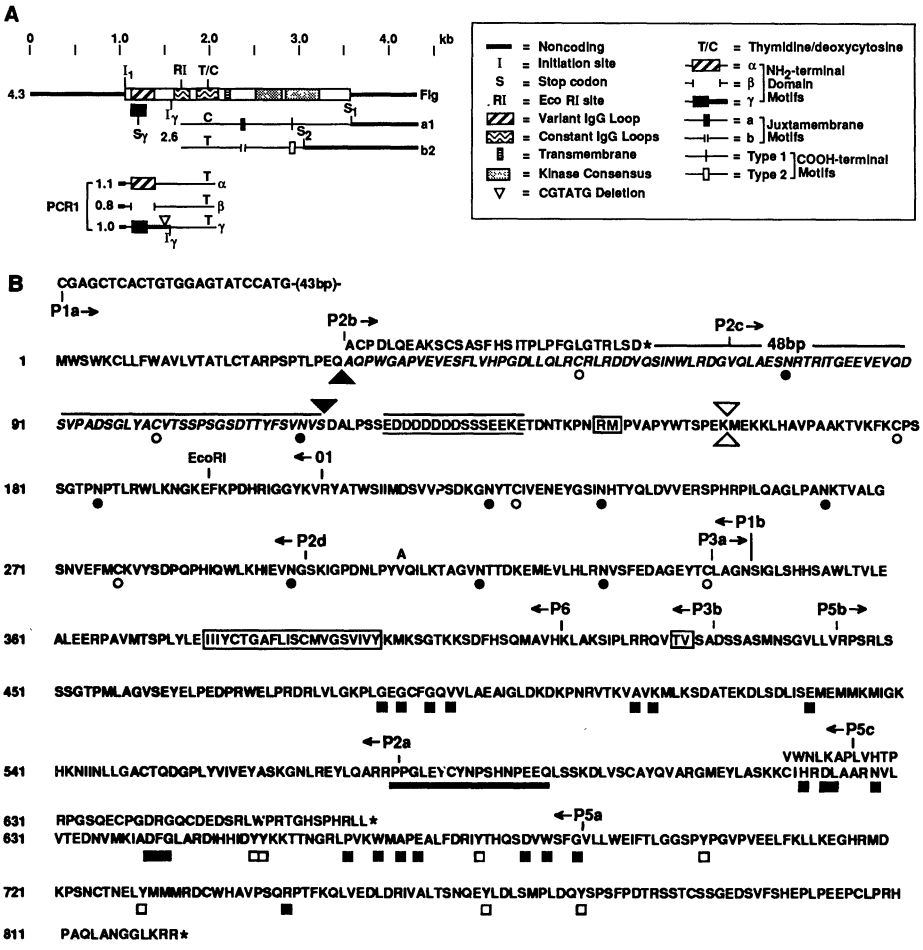

Fig. 1. HBGF receptor cDNAs from HepG2 cells. (**A**) Schematic of full-length (*flg*) cDNA for HBGF-Rαa1 (Fig. 2B). The single Eco RI site and the single base pair T/C variant is indicated. I_1 indicates the common predicted translational initiation site for α, β, and γ motifs, and I_γ indicates the alternate predicted initiation site for the γ motifs. S_γ, S_1, and S_2 indicate the stop codons that determine the γ and type 1 and 2 motifs, respectively. Partial cDNAs are indicated in kilobase pairs. (**B**) Deduced amino acid sequence of *flg* HBGF-R variants. The complete sequence of HBGF-Rαa1 (Fig. 2B) preceded by the 67 5′-noncoding nucleotides containing the 5′ primer P1a is indicated. Positions of PCR primers (*9*) are indicated at their 5′ ends. The IgG-like disulfide loop of α is italicized. The unique 31-aa γ sequence, which is in-frame with the common initiation and secretory signal, and the following 48-bp noncoding nucleotide sequence (solid line) in the 144-bp γ insert is indicated over the HBGF-Rαa1 sequence. Asterisks indicate stop codons. The characteristic acidic residues are overlined and underlined. Site of the CGTATG deletion in the γ cDNA that codes for Arg-Met in the α and β sequences is boxed. Closed triangles indicate insertion sites of the 267-bp and 144-bp nucleotide sequences that define the α and γ variants. Open triangles indicate alternate candidate translational initiation site (γ); open circles indicate cysteines that may form disulfides in the IgG-like loops; closed circles indicate putative glycosylation sites. The Val to Ala variant (aa 308) and the transmembrane domain (aa 377–397) is indicated. The Thr-Val variation (aa 428–429) in the juxtamembrane domain is boxed. Closed boxes indicate conserved tyrosine kinase consensus residues. The interkinase domain is underlined. The unique 44-aa residues (VWNLKAPLVHTPRPGSQECPGDRGQCDEDSRLWPRTGHSPHRLL) that define the type 2 COOH-terminus are shown over the type 1 COOH-terminus. Open boxes indicate unique potential tyrosine phosphorylation sites in the type 1 COOH-terminus. Complete nucleotide sequences have been submitted to GenBank.

nus. Linkage of the a-type juxtamembrane motif and type 2 COOH-terminus was confirmed by sequencing two independent clones. Of the 173 clones that potentially coded for the b-type juxtamembrane motif (negative in the P3a-P3b screen above), 49 were then screened with a common 5′ primer (P5b) and the type 2–specific 3′ primer (P5c). Forty-five clones exhibited the 0.5-kb fragment, indicative of presence of the coding sequence for the type 2 COOH-terminus. The four remaining doubly negative clones from the P3a-P3b and P5b-P5c screens coded for the b-type juxtamembrane and the type 1 COOH-terminal motifs. Thus, the b-type juxtamembrane motif was linked to both COOH-terminal motifs.

These results show that multiple species of HepG2 mRNA code for combinations of three distinct structural domains: three motifs in the NH_2-terminal domain (α, β, and γ); two distinct juxtamembrane sequences (a and b); and two COOH-terminal structures (type 1 and 2). A minimum of 6 and theoretical maximum of 12 forms of *flg*-related gene products may be expressed in a single differentiated liver tumor–derived cell population (HepG2) (Fig. 2B). Intensities of PCR bands and frequency of appearance in cloned cDNAs suggested that the b-type juxtamembrane and the type 2 COOH-terminal motifs were the most abundant in HepG2 cells. The α, β, and γ NH_2-terminal motifs appeared at equal frequencies. Analysis of cDNAs that extend from the coding sequence for the NH_2-terminal to the COOH-terminal motifs and domain-specific antibodies to translation products will be necessary to determine relative expression of the 12 potential variants in a single cell or tissue.

We next sought to determine if the NH_2-terminal domain structures in human hepatoma *flg*-related cDNAs formed HBGF binding sites. Thus, we constructed mammalian cell expression plasmids (P91023B) (*10*) that contained cDNAs that encoded for the α, β, and γ NH_2-terminal motifs fused to coding sequence for the common transmembrane domain and 18 residues of the juxtamembrane region. The constructions were transfected into a monkey kidney cell line (COS), and ligand-binding [^{125}I-labeled HBGF-1 (acidic FGF) and ^{125}I-labeled HBGF-2 (basic FGF)] to the transfected COS cells was analyzed by Scatchard plot (Fig. 3A) and covalent ligand affinity cross-linking (Fig. 3, B to D). Scatchard analysis indicated that cells transfected with cDNA coding for the α and β loop structures exhibited a 15- and 25-fold increase in HBGF binding sites per cell with an apparent dissociation constant (K_d) of 400 to 800 pM (*11*). Affinity cross-linking analyses of cells transfected with cDNAs coding for the α and β extracellular domains resulted in labeled bands

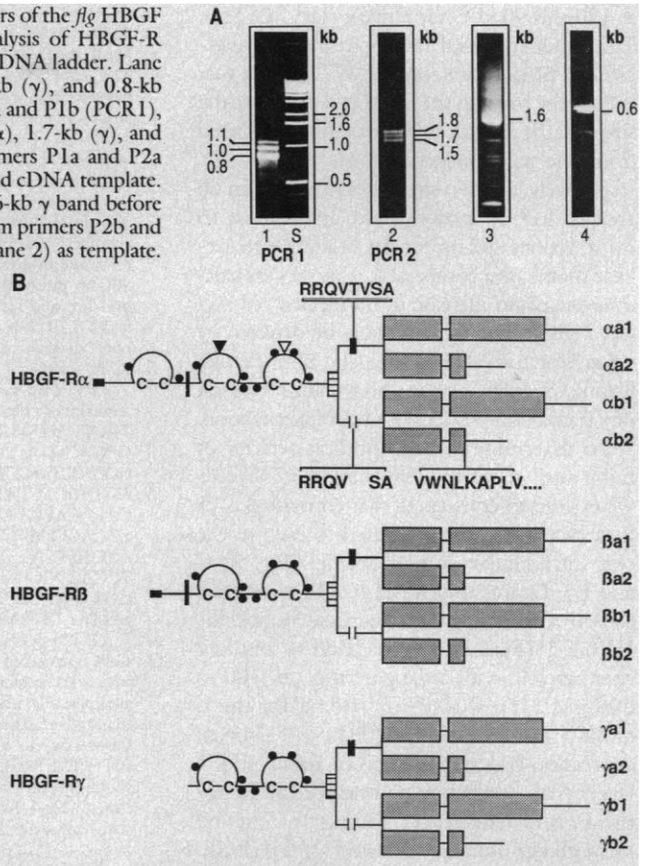

Fig. 2. Identification of members of the *flg* HBGF receptor family. (**A**) PCR analysis of HBGF-R cDNAs. S indicates a standard DNA ladder. Lane 1 shows the 1.1-kb (α), 1.0-kb (γ), and 0.8-kb (β) bands between primers P1a and P1b (PCR1), and lane 2 shows the 1.8-kb (α), 1.7-kb (γ), and 1.5-kb (β) bands between primers P1a and P2a (PCR2) with HepG2 first strand cDNA template. Lane 3 shows the amplified 1.6-kb γ band before purification, which resulted from primers P2b and P2a with the PCR2 product (lane 2) as template. Lane 4 shows the P2c-P2d band (0.6 kb) with a γ cDNA clone template. Reaction mixtures (50 μl) contained 10 mM tris-HCl (pH 8.3), 50 mM KCl, 1.5 mM $MgCl_2$ 0.1% gelatin, 1.25 units of *Taq* polymerase (Perkin-Elmer Cetus) and 0.20 mM each of deoxyadenosine triphosphate (dATP), deoxycytosine triphosphate (dCTP), deoxyguanosine triphosphate, and thymidinetriphosphate. Template and primer concentrations (0.75 to 75.0 pmol) were optimized for each condition. First strand cDNAs were synthesized with independent preparations of HepG2 polyadenylated RNA as template. PCR1 and PCR2 were performed for 40 cycles at 94°C for 1 min, 55°C for 2 min, and 72°C for 3 min. All others were carried out for 30 cycles at 94°C for 1 min, 60°C for 1 min, and 72°C for 1 min. PCR fragments were analyzed and purified on 1% agarose gels, cloned into SK Bluescript phagemide vector (Stratagene), and individual clones were purified and identified by plasmid mini-preparation. (**B**) Twelve possible variants of the HBGF receptor in HepG2 cells. The predicted α, β, and γ NH_2-terminal motifs are shown fused to the a and b juxtamembrane sequence variants and the type 1 and 2 COOH-termini. Filled box, the common initiation site and signal sequence for α and β motifs; filled circles, potential glycosylation sites; filled rectangles, acidic-rich sequence; lined rectangles, the transmembrane domain; hatched boxes, tyrosine kinase consensus sequences; open inverted triangle, TC:Val/Ala site; closed inverted triangle, the Eco RI site.

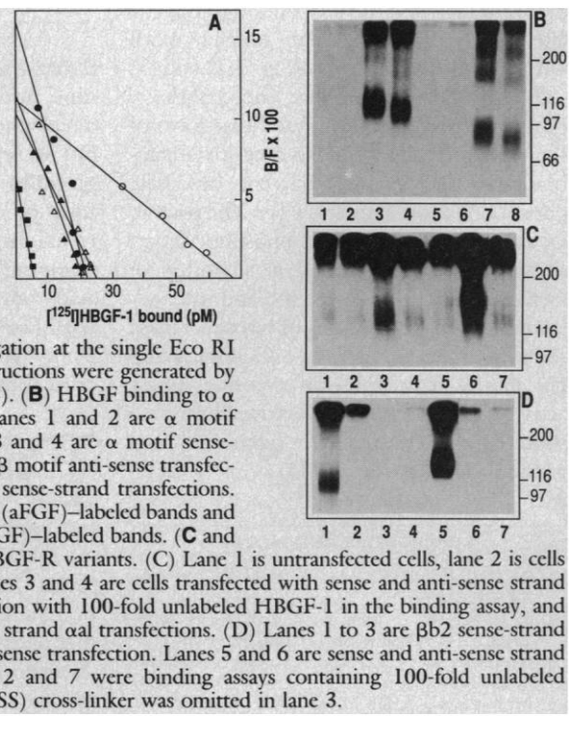

Fig. 3. Analysis of HBGF binding activity of the cloned receptors. (**A**) Representative Scatchard analyses. COS-1 cells transfected with the β extracellular domain (○), αa1 (△), αb2 (▲), βb2 (●) and vector alone (■) exhibited apparent K_d's of 600, 250, 180, 140, and 90 pM, respectively. Scatchard analysis was performed on suspended COS-1 cells and ligand affinity cross-linking analysis on monolayer cells in assays containing 625 pM ^{125}I-labeled ligand. Full-length cDNAs were constructed from 5′ and 3′ cDNAs by ligation at the single Eco RI site. The NH_2-terminal domain constructions were generated by PCR with Pla and P6 primers (Fig. 1B). (**B**) HBGF binding to α and β extracellular domain motifs. Lanes 1 and 2 are α motif anti-sense strand transfections, lanes 3 and 4 are α motif sense-strand transfections, lanes 5 and 6 are β motif anti-sense transfections, and lanes 7 and 8 are β motif sense-strand transfections. Lanes 1, 3, 5, and 7 are [^{125}I]HBGF-1 (aFGF)–labeled bands and lanes 2, 4, 6, 8 are [^{125}I]HBGF-2 (bFGF)–labeled bands. (**C** and **D**) HBGF-1 binding to full-length HBGF-R variants. (C) Lane 1 is untransfected cells, lane 2 is cells transfected with empty vector, and lanes 3 and 4 are cells transfected with sense and anti-sense strand αb2 cDNA. Lane 5 is an αa1 transfection with 100-fold unlabeled HBGF-1 in the binding assay, and lanes 6 and 7 are sense- and anti-sense strand αa1 transfections. (D) Lanes 1 to 3 are βb2 sense-strand transfections, and lane 4 is a βb2 anti-sense transfection. Lanes 5 and 6 are sense and anti-sense strand βa1 transfections, respectively. Lane 2 and 7 were binding assays containing 100-fold unlabeled HBGF-1. Disuccinimidyl suberate (DSS) cross-linker was omitted in lane 3.

at 120 and 90 kD, respectively (Fig. 3B) (*12*). This result indicated that both motifs are expressed as products on the cell surface that encode the binding site for HBGF. Because the sizes of the extracellular structures predicted from the aa sequence are 44 and 34 kD, respectively, the two structures may contain 60 and 40 kD of carbohydrate. In contrast to constructions coding for the α and β extracellular motifs, the comparable γ motif construction caused no increase in transfected cell surface HBGF binding that could be detected by either Scatchard analysis or ligand affinity cross-linking. Stability, activity, and cellular location of γ translation products is under investigation.

To determine HBGF binding activity of full-length receptor isoforms, in COS cells we expressed constructs that contained α or β extracellular domains fused to each of the two intracellular domain motifs (Fig. 3, C and D). Expression of full-length constructs caused a 5- to 15-fold increase in specific HBGF-1 (Fig. 3A) and HBGF-2 binding sites per cell, with an apparent K_d of 100 to 500 pM (*11*). Constructs coding for the α motif yielded [^{125}I]HBGF-1–labeled expression products that were about 30 kD larger than constructs coding for the β motif. Finally, constructs coding for the b2 intracellular domain exhibited [^{125}I]HBGF-labeled expression products that were about 20 kD smaller than constructs coding for the a1 intracellular domain (*13, 14*).

The three distinct structural domains that combine to form HBGF receptor isoforms are likely to affect ligand binding, oligomerization, cellular location, metabolism, and signal transduction (*15*). The α and β extracellular motifs appear to differentially oligomerize (*12*), and ligand binding may be affected by the intracellular domain motif with which it is combined (Fig. 3, C and D) (*12, 13*). The cDNA that encodes the γ motif may result in an intracellular form of the receptor. The a- and b-type juxtamembrane motifs contain different candidate phosphorylation sites for a Ser-Thr protein kinase. Juxtamembrane phosphorylation sites have been implicated in alteration of ligand affinity, kinase activity, and internalization (down-regulation) of tyrosine kinase receptors (*15, 16*). The two COOH-terminal motifs may differ in tyrosine kinase activity, in interaction with intracellular substrates, and as substrates for tyrosine kinases in the COOH-terminus (*15*).

REFERENCES AND NOTES

1. W. H. Burgess and T. Maciag, *Annu. Rev. Biochem.* **58**, 575 (1989).
2. P. L. Lee, D. E. Johnson, L. S. Cousens, V. A. Fried, L. T. Williams, *Science* **245**, 57 (1989).
3. M. Ruta *et al.*, *Proc. Natl. Acad. Sci. U.S.A.* **86**, 8722 (1989).
4. M. Kan *et al.*, *J. Biol. Chem.* **263**, 11306 (1988).
5. M. Kan *et al.*, *Proc. Natl. Acad. Sci. U.S.A.* **86**, 7432 (1989).
6. M. Ruta *et al.*, *Oncogene* **3**, 9 (1988).
7. The 1.8-, 1.1-, and 0.6-kb clones, identified by hybridization with an oligonucleotide (01) in the 5′ sequence of a1 and a2 cDNAs (Fig. 1B), overlapped a1 and b2 cDNAs by 178, 53, and 96 nucleotides, respectively. The 1.8-kb cDNA, when ligated to a1 or b2, represents a near full-length 4.2-kb mRNA that encoded a three–IgG-like loop extracellular domain (α) (Fig. 1). The 1.1- and 0.6-kb cDNAs exhibited a deletion of 267 bp that encoded the 89-residue outermost IgG-like loop (Fig. 1). The 306-bp preceding the common translational initiation site and secretory signal sequence in the 1.1- and 1.8-kb cDNAs were identical. The remaining 5′ noncoding sequences were unique.
8. R. K. Saiki *et al.*, *Science* **230**, 1350 (1985).
9. The P1a primer sequence is indicated in Fig. 1B. The sequence of other primers was as follows: P2b, GCTTGCCCAGATCTCCAG; P2c, CCTGCTCTGCTGGAGAGGAAC; 01, GACCTTGTAGCCTCC; P2d, CCCATTCACCTCGATGTGCTT; P3a, TTGGCGGGTAACTCTATCGGACTC; P1b, GTTACCCGCCAAGCACGTATAC; P6, TATATGAATTCGTGCACAGCCATCTGGCTGTGGAA; P3b, AGCAGACACTGTTAC; P5b, CGGCCATCACGGCTCTCCTCCAGTGGCG; P2a, GGGCCTCCGGGCCTGCAGGTACTCCG; P5c, GAGCCTTCAGGTTCCACA; and P5a, CGAAAGACCACACATCA.
10. G. G. Wong *et al.*, *Science* **228**, 810 (1985).
11. Cells transfected with the extracellular domain constructions exhibited a higher number of binding sites per cell with higher apparent K_d (lower affinity) than cells transfected with full-length constructions. Otherwise, no consistent difference in apparent K_d for HBGF binding has been demonstrated among receptor isoforms by Scatchard analysis. Untransfected COS cells displayed about 4000 sites per cell with apparent K_d of 100 pM. Since COS cells express uncharacterized receptor isoforms, the apparent K_d is likely a composite of host cell and transfected receptor species.
12. Although cross-linking artifact cannot be eliminated, higher molecular size species of ligand-receptor complexes may indicate self-oligomerization or activation and association of transfected products with host cell receptor species. Oligomeric bands are more apparent in cells transfected with β constructs, independent of COOH-terminus (Fig. 3) (J. Hou *et al.*, unpublished data).
13. Constructions that coded for the a1 intracellular domain exhibited more intensely HBGF-labeled species than the b2 motifs, as evident in Fig. 3, C and D. Separate experiments with b1 and a2 constructions in permanently transfected cells indicated that the reduced ligand-binding is due predominately to the b juxtamembrane motif and to a lesser extent, the type 2 COOH-terminal motif, independent of extracellular domain (J. Hou *et al.*, in preparation).
14. Untransfected COS cells exhibited a single HBGF-labeled band at 150 kD. HepG2 cells displayed labeled bands of 120, 150, and 280 kD, the most intense of which was 120 kD.
15. A. Ullrich and J. J. Schlessinger, *Cell* **61**, 203 (1990).
16. H. Hoshi *et al.*, *FASEB J.* **2**, 2797 (1988).

17. We thank E. Mansson, S. Harris, and S. Goodrich for advice and synthesis of oligonucleotides, M. Mueckler for the HepG2 λgt11 phage library, E. Shi for assistance in [^{125}I]HBGF labeling, J. Huang and F. Wang for assistance in analysis of cDNA clones, and D. Fast and M. Kan for assistance in culture of HepG2 cells. Supported by grants from the U.S. National Institutes of Digestive and Kidney Diseases and the National Cancer Institute.

25 July 1990; accepted 7 November 1990

Inability of Malaria Vaccine to Induce Antibodies to a Protective Epitope Within Its Sequence

YUPIN CHAROENVIT, WILLIAM E. COLLINS, TREVOR R. JONES, PASCAL MILLET, LEO YUAN, GARY H. CAMPBELL, RICHARD L. BEAUDOIN, J. ROGER BRODERSON, STEPHEN L. HOFFMAN*

***Saimiri* monkeys immunized with a recombinant protein containing 20 copies of the nine amino acid repeat of the *Plasmodium vivax* circumsporozoite (CS) protein developed high concentrations of antibodies to the repeat sequence and to sporozoites, but were not protected against challenge. After intravenous injection of an immunoglobulin G3 monoclonal antibody (NVS3) against irradiated *P. vivax* sporozoites, four of six monkeys were protected against sporozoite-induced malaria, and the remaining two animals took significantly longer to become parasitemic. Epitope mapping demonstrated that NVS3 recognizes only four (AGDR) of the nine amino acids within the repeat region of the *P. vivax* CS protein. The monkeys immunized with $(DRA^{A}_{D}GQPAG)_{20}$ did not produce antibodies to the protective epitope AGDR. Thus, determination of the fine specificity of protective immune responses may be critical to the construction of successful subunit vaccines.**

DURING RECENT YEARS THERE HAS been considerable effort to produce vaccines designed to induce protective antibodies against repetitive sequences on the CS protein of *Plasmodium*, which causes human malaria. These efforts have been, in large part, based on the observation that passive transfer of monoclonal antibodies against the CS protein of rodent parasites *Plasmodium berghei* (*1, 2*) and *P. yoelii* (*3*) protects against challenge with sporozoites. Incubation of *P. falciparum* or *P. vivax* sporozoites with Fab fragments of monoclo-

Y. Charoenvit, T. R. Jones, L. Yuan, R. L. Beaudoin, S. L. Hoffman, Infectious Diseases Department, Naval Medical Research Institute, Bethesda, MD 20889.
W. E. Collins, P. Millet, G. H. Campbell, J. R. Broderson, Malaria Branch, Centers for Disease Control, Atlanta, GA 30333.

*To whom correspondence should be addressed.